Gabbro layering induced by simple shear in the Oman ophiolite Moho transition zone

David Jousselin, Luiz F.G. Morales, Marie Nicolle, Aurore Stephant

Gabbro layering induced by simple shear in the Oman ophiolite Moho transition zone

David Jousselin, Luiz F.G. Morales, Marie Nicolle, Aurore Stephant

Gabbro layering induced by simple shear in the Oman ophiolite Moho transition zone

David Jousselin[1], Luiz F. G. Morales[2], Marie Nicolle[1], and Aurore Stephant[1]

1: Université de Lorraine, CRPG, 54501 Vandoeuvre les Nancy, France

2: Deutsches GeoForschungsZentrum (GFZ), Section 3.2 Telegrafenberg, 14473, Potsdam, Germany

Abstract

We investigate the origin of modal layering in gabbro lenses of the Moho transition zone in the Oman ophiolite with a microstructural study. Gabbro lenses exhibit a shape preferred orientation of plagioclase crystals, that are euhedral and devoid of any intracrystalline deformation. This texture and field kinematic indicators show a strong simple shear deformation in magmatic conditions. The parallelism of the lineation in gabbros and the plastic lineation of the host dunite indicate that their development is contemporaneous, and that the magmatic features are passively coupled to the solid-plastic flow of the host mantle. We also found undeformed-isotropic and weakly deformed-roughly layered gabbro. The host rock is plagioclase and clinopyroxene impregnated dunite; it contains euhedral plagioclase suggesting that some grains crystallized in suspension. There is no clear boundary between the gabbro and the host rock; on the contrary, the limit is diffuse, with increasing plagioclase and clinopyroxene content from the dunite to the gabbro over tens of meters. This suggests that the gabbro corresponds to melt impregnated dunite. We defined 4 gabbro types, from unlayered (type 1) to well layered (type 4) with progressively more continuous and distinct layers. We characterized deformation with crystal shape and crystallographic preferred

orientation (CPO) measurements. Unlayered samples have a random fabric; type 2 have a very weak shape fabric and planar CPO, defined by olivine and plagioclase (010) planes; type 3 have a weak fabric, with a lineation defined by the [001] olivine axis and the [100] plagioclase axis, which reflects the shape fabric; type 4 have a strong shape fabric and CPO, with a lineation defined by the [100] olivine and plagioclase axis. We interpret the progression from isotropic to clear S-L fabrics as a result of increasing deformation imposed by the flowing host mantle. The type 2 gabbros must result from compaction; with increasing simple shear, the lineation is developed in type 3 samples; finally, with lower melt content, suspension flow switches to plastic deformation in the olivine-rich layers, leading to plastic olivine fabrics in type 4 samples. We deduce that layering originates from simple shear, which other studies show induces strong segregations in suspended particles, and plastically deformed rocks. To build the isotropic stage, melt must accumulate faster than the deformation, suggesting that melt is extracted by dikes.

1. Introduction

Layering in igneous rocks is a focal issue because it is related to magma emplacement and evolution. Modally layered gabbros in ophiolites are regarded as relics of the low velocity zone beneath the axial melt lens reported at fast oceanic spreading ridges (e.g. Detrick et al, 1987; Caress et al, 1992), and represent a key section in the ridge melt plumbing system. Several models have been proposed to explain the formation of layered gabbro in ophiolites. The earliest models advocated the accumulation of crystals in a magma chamber (e.g. Smewing, 1981); others proposed that layering results from the tectonic transposition of melt either sinking from above as it crystallizes from the melt lens (Quick and Denlinger, 1993 known as the "glacier model") or flowing from beneath as it is extracted from the mantle

(Nicolas et al, 1988). The model of Henstock et al (1993) is a variation of the gabbro glacier model where layering originates from cyclic melt sills rather from than sedimentation at the bottom of a permanent melt lens followed by deformation. Alternatively, layers may represent stacked sill intrusions (Boudier et al, 1996a; Kelemen et al, 1997a; Lissenberg et al, 2004; known as "sheeted sill model"). No consensus emerges from these models, each implies different melt paths, times of residence and extents of interaction with the host rock. One problem that hinders our knowledge of the origin of modal layering is that we see only the final products, i.e. the layered gabbros, and have no trace of evolutional stages since the melt was first emplaced. This may be because transitional stages are brief relative to geological time scales, and thus are rarely fossilized. The Oman ophiolite may enable to capture such short lived processes which could have occurred at the ridge axis itself. Mapping of mantle diapirs and dike distribution show that a spreading axis which produced a 50 Km wide portion of oceanic crust -similar to that of fast spreading-ridges- is preserved in the southern massifs (Ceuleneer et al, 1988; Boudier et al, 1997). The Moho transition zone (MTZ) in the Oman ophiolite is a few meters to a few hundreds meters thick, and is characterized by gabbro lenses imbedded in dunite, plagioclase and clinopyroxene impregnated dunite, and depleted harzburgite (Boudier and Nicolas, 1995). Identification of this unit as the uppermost mantle is based on the recognition of mantle fabrics and the occurrence of residual orthopyroxene in the MTZ, showing that dunite results from dissolution of harzburgite pyroxene by a circulating melt (Sinton, 1977; Nicolas, and Prinzhofer, 1983). The gabbro lenses in the MTZ are indistinguishable from layered gabbros in the lower crust; they have the same type of modal layering and chemical composition (Kelemen et al, 1997a), which suggests that they formed in the same way. The presence of melt at the MTZ is now recognized by a growing number of marine geophysical studies at fast and intermediate spreading ridges (Garmany, 1989; Crawford and Webb, 2002; Nedimovic et al, 2005), underscoring the importance of

76 understanding the structure of the MTZ. This paper presents new field observations and a
77 microstructural study of gabbroic rocks in the MTZ associated with the well-known Maqsad
78 mantle diapir (Ceuleneer et al, 1988; Jousselin et al, 1998). We distinguish four types of
79 samples which represent different evolutionary stages of the gabbro layering. Because
80 universal-stage measurements are time consuming and tedious to acquire, especially for
81 plagioclase, published crystallographic preferred orientation (CPO) data in Oman layered
82 gabbro are limited to seven examples dispersed in four studies: one in Benn and Allard, 1989;
83 three in Boudier and Nicolas, 1995; one in Boudier et al, 1996a with olivine only; two in
84 Yaouancq and MacLeod, 2000, with plagioclase only; the latter also contain fabric data for
85 six foliated gabbros of the unlayered upper part of the gabbro section. Of the five olivine
86 CPOs, two are in MTZ gabbro lenses (Boudier and Nicolas, 1995), the others are in the crust.
87 Fifteen more plagioclase fabrics were measured in studies devoted to anorthosite layers in the
88 foliated upper crust (Morales et al, 2011). The use of a scanning electron microscope (SEM)
89 equipped with an electron back-scattered diffraction (EBSD) system allowed us to gather a
90 dataset of 27 olivine CPOs and 35 plagioclase CPOs. The acquisition of this unprecedented
91 dataset was essential to reveal possible deformation stages within the different types of
92 gabbro observed. We also characterized deformation by crystal shape preferred orientation
93 measurements in 7 thin sections. Deformation analysis coupled to sample distribution, and
94 description of the layering, permit us to discuss the origin of gabbro layering and magma
95 extraction processes.
96
97 **2. Geological stetting and field observations**
98
99 The MTZ in ophiolites represents a level where part of the melt extracted from the mantle is
100 collected, circulates and partially crystallizes, before feeding the overlying oceanic crust

(Karson and Collins, 1984; Boudier and Nicolas, 1995; Sano and Kimura, 2007). It offers the opportunity to observe the distribution of melt ponding and percolating in a deforming matrix. In the Oman ophiolite, the development of a thick (>100 meters) MTZ is related to the presence of mantle diapirs that carry the melt from below (Nicolas, et al, 1996; Godard et al, 2000). The Maqsad mantle diapir region has been extensively studied, providing a well-known general framework for detailed studies of the MTZ and layered gabbro lenses (Rabinowicz et al, 1987; Ceuleneer et al, 1988; Boudier and Nicolas, 1995; Kelemen et al, 1997a; Jousselin et al, 1998; Koga et al, 2001). The crust-mantle interface (Moho) in this area is nearly horizontal, and dikes in the sheeted dike system are vertical. The region can thus be viewed as a paleospreading center dissected by erosion, without any subsequent deformation.

Gabbro lenses in the MTZ are always magmatically deformed (i.e. with a grain shape preferred orientation of anisometric and euhedral crystals ascribed to flow in the dense suspension; e.g. Benn and Allard, 1989; Nicolas, 1992; Yaouancq and MacLeod, 2000), without sample-scale evidence of plastic deformation (such as augen pyroxene grains), and are usually subhorizontal. Lens thickness varies from a few centimeters to tens of meters, with a horizontal extent of a few meters to a hundred meters; many lenses are < 1m thick, and some tend to cluster in the upper part of the MTZ. Layer thicknesses vary from a few millimeters to a few tens of centimeters. Graded layers are common features (about 20-25% of 200 layers in outcrops of our field study), but the strong majority of individual layers tend to be homogeneous from the base to the summit, with sharp limits at each boundary. Bulk and layer composition are variable. Leucotroctolite bulk compositions seem dominant and clinopyroxene-rich layers seem more rare than those rich in olivine or plagioclase. Table 1 shows representative variations of the layer composition. Although we are not aware of any rigorous systematic measurements of lens and layer dimensions and modal compositions, our

observations agree with field impressions and the few sample descriptions provided by other workers (Boudier and Nicolas, 1995; Boudier et al, 1996a; Kelemen et al, 1997a; Korenaga et al, 1997). Nevertheless, the presence of several tens of meters thick lenses, and the relative importance of graded layers (qualified as an important feature in Kelemen et al, 1997a), seem overestimated. All structural features are generally concordant: the contact of gabbro lenses with the host dunite, modal layering (Fig. 1), and the gabbro magmatic foliation and lineation are all usually parallel to the asthenospheric plastic foliation and lineation of the host dunite. However several outcrops with less deformed gabbros show semi-discordant lenses with irregular shapes and rough layering, or discordant layers, and a few outcrops show isotropic gabbros, troctolites, and olivine-rich troctolite patches (Fig. 2). In particular, one outcrop (N22°59'32", E57°59'46", called hereafter the Khilah outcrop) presents a spectacular case of mostly isotropic gabbros, extending over five hundred meters (Fig. 3). The outcrop contains a few 1 to 20 meters wide zones with poorly layered gabbros. When it is present, layering is parallel to the plastic foliation of the host peridotite observed 20 to 100 meters away. Except for the roughly layered zones, and a few randomly oriented heterogeneities (mainly centimeter sized dunite bodies) (Fig. 2B), the gabbro seems a relatively homogeneous mix of plagioclase (60-80%), olivine (10-30%) and clinopyroxene (0-20%) (Fig. 2A). The transition from the host peridotite (mainly plagioclase and clinopyroxene impregnated dunite) to the isotropic gabbro is diffuse, with increasing plagioclase and clinopyroxene impregnations towards the center of the outcrop over few meters. In parts of the impregnated dunite, plagioclase crystals are automorphic, suggesting that there was enough melt for the crystals to grow in suspension (Fig. 4A). When plagioclase and clinopyroxene reach 25%, they contour and isolate olivine grains in dunite and the rock becomes isotropic (Fig. 4B). This near poikilitic texture (with olivine crystals larger than oikocrysts) gives way to phaneritic textures

with a hypidiomorphic granular fabric when the plagioclase and clinopyroxene fraction increases and the rock becomes a gabbro.

The general characteristics of gabbro lenses bear similarities with those of plagioclase and clinopyroxene impregnations in the MTZ dunite (Fig 5). In the impregnated dunite, clinopyroxene and plagioclase grains are devoid of any intracrystalline deformation, but they have an elongated shape, parallel to the plastic stretching lineation of the host dunite, with more elongated grains, and stronger shape preferred orientation associated with the stronger olivine CPOs in the dunite, suggesting crystals filled melt pockets which shape was governed by strain (Jousselin and Mainprice, 1998). As for the layered gabbro lenses versus the isotropic gabbro, field observations of well transposed melt impregnations parallel to the foliated dunite are much more common than isotropic impregnations within poorly foliated dunite; however isotropic impregnations are not rare. All strongly elongated impregnations occur in dunite whereas some of the untransposed ones occur in residual harzburgite, where a few corroded orthopyroxene grains can be observed. Some of the impregnations are continuous with the tip of gabbro lenses or form diffuse contacts with gabbro lenses (Fig. 5; figure 1a in Boudier et al, 1996a) suggesting that they are cogenetic.

3. New structural observations, and kinematic analysis

Kelemen et al. (1997a) assume that deformation by simple shear would have obliterated graded layers, and conclude that most deformation must have been pure shear (flattening during compaction). This would suggest that the gabbro lenses were not affected by the surrounding mantle flow and therefore would be late or off-axis features, whereas their study rightfully points to chemical compositions that argue that the lenses were emplaced on-axis.

However, we find numerous and robust indicators that gabbro lenses and the host rock recorded a strong simple shear deformation (Fig. 6), except for the local isotropic zones aforementioned: (i) well developed lineation in the foliation plane, (ii) folds in the gabbro lenses with an axis consistently parallel to the lineation (Fig. 6A-B), (iii) synmagmatic normal faults with an azimuth at high angle with the magmatic lineation and S/C shear bands (Fig 6C-D; Nicolas, 1992), (iv) the frequent CPO measurements in the host dunite, that show [100] crystallographic axis of olivine at a small angle to the lineation (Fig. 7A; Ben Ismaïl and Mainprice, 1998; Dijkstra et al, 2002). In some cases, an obliquity of the olivine and plagioclase shape preferred orientation with the layering is discernible (Fig. 6E). This evidence indicates moderate simple shear deformation, but in most cases, all structures are parallel, pointing to a very large strain, including in the graded layers (Nicolas, 1992). It should also be noted that a 50% compaction, as calculated by Browning (1984) and used by Kelemen et al (1997a), seems insufficient to produce a strong foliation (Higgins, 1991). The parallelism of the shape fabric in melt impregnated dunite, the magmatic lineation in gabbros, and the plastic lineation of the host dunite, indicate that their development is contemporaneous, and that the magmatic features are passively coupled to the plastic flow of the surrounding peridotitic matrix.

4. Microstructural analysis

4.1. Gabbro layering and shape preferred orientation

We present a microstructural study of samples of the MTZ, with an emphasis on the preserved cases of isotropic gabbros, and weakly layered samples that may represent the earliest subsequent stages of evolution, and which have not been studied before. We have studied 10

samples in the Khilah outcrop, and 52 others in its vicinity (Fig 3). Four types of samples were distinguished: type 1 is characterized by the absence of layering (Fig. 2A-B); type 2 shows weakly defined layers which can be followed over few centimeters (Fig. 2C-D); type 3 shows more strongly defined layers, still with diffuse or wavy limits (Fig.2E-F); the more common type 4 corresponds to the presence of very well defined layers with sharp and straight limits (Fig.1). Type 3 layers can rarely be followed over two meters, and type 4 layers may be followed over several meters. All samples display a magmatic texture; plagioclase show euhedral magmatic laths, and a few are twinned, which implies sufficient freedom for crystals to rotate without undergoing plastic deformation. Clinopyroxene is tabular or round-shaped with no evidence of deformation. In type 1-3 samples, some of the olivine grains show clear crystallographic faces suggesting a cumulative origin, or overgrowth around the edges of mantle xenocrysts (Boudier, 1991). In all samples, olivine does not show any dynamic recrystallization, but some grains have undulose extinction suggesting light plastic deformation. Field observations of crystal alignment and aggregate elongation indicate that deformation increases from type 1 to type 4 samples. To evaluate the importance of the shape fabric, we performed shape preferred orientation analyses based on hand drawings of seven thin sections, sectioned parallel to the lineation and perpendicular to the magmatic foliation (XZ plane). Two type 1 samples were analyzed; as no foliation and lineation is visible in these, the thin sections were cut parallel to the orientation of the nearest observable XZ plane from nearby outcrops. For each crystal, we measured the longest chord connecting any two points on the perimeter, and the orientation of this axis with respect to the X axis. As anticipated, the two type 1 samples do not show any crystal shape preferred orientation; this was also checked on a thin section cut perpendicularly; preferred orientation in type 2 to 4 gradually changes from weak to strong (Fig 7B).

4.2. Crystallographic preferred orientation

Of sixty-two gabbro samples we collected, forty were chosen on the basis of their type variety and freshness for CPO analysis. Phases and orientation were mapped using the SEM-EBSD facility at Geosciences Montpellier (e.g. Fig. 1C) with a 45-100 μm grid spacing. Due to alteration or lack of a mineral phase, we obtained 27 olivine CPO and 35 plagioclase CPO usable measurements (100 measured grains per phase, except 5 cases with >75 measured grains which were considered valid because the olivine fabric seemed unambiguous. Pole figures are plotted with one point per grain. Grain counting was done manually, because automatic counting from the map counts a single grain as several when it is cut by veins). Alteration is particularly important in our weakly deformed samples, which choice is more limited than for the type 4 samples; thus to reflect the variety of the microstructures while insuring that enough grains are measured to obtain a valid CPO, eight parallel thin sections were cut for two type 2 samples, and representative CPOs were obtained once the measurements were compiled. Our study also includes 2 olivine CPOs in the MTZ host dunites, measured with a universal stage. A selection of representative CPOs of olivine and plagioclase is shown in Fig. 7; the full CPO dataset is available in online Supplementary Information, including samples with specific patterns described below.

The two type 1 samples show random CPOs. The five type 2 samples show essentially planar fabrics, where the (010) crystal faces of olivine and plagioclase define the magmatic foliation. The type 2 olivine fabric is not regular, one seems random (07OD21B), in the other cases the [001] axis draws a girdle in the foliation plane, and the [100] axis orientation is erratic, except for one case (07OD44E) where it draws a girdle in the foliation plane. The plagioclase fabric is better defined, with the [100] axis drawing a girdle in the foliation plane, even defining a

weak lineation in two cases (07OD21B and 10-OM43I); the [001] axis orientation is imprecise, with a light tendency to lie in the foliation plane (clear for one sample: 07OD32). The type 3 samples have a more consistent CPO; both olivine (4 samples) and plagioclase (5 samples) show a lineation superimposed on the (010) foliation. In olivine, the [001] axis corresponds to the lineation, while [100] is perpendicular to it; in plagioclase, [100] corresponds to the lineation, and [001] has a somewhat erratic orientation. The type 4 samples have the same plagioclase CPO as type 3 samples; however, olivine fabrics are drastically different with very well defined [100] (010) CPOs, and a weak tendency of the [001] axes to concentrate near the Y axis, with one exception showing a [100] (001) fabric (10-OM42G3). Olivine CPOs in the host dunite show the classic [100] (010) mantle fabric (Ben Ismaïl and Mainprice, 1998).

5. Interpretation and discussion

5.1. Comparison with sill models

The model where modally layered gabbro of the lower crustal section formed in sills (Boudier et al, 1996; Kelemen et al, 1997a) is inferred on the analogy with gabbro lenses of the MTZ that are interpreted as sill intrusions. This interpretation relies on the common elongated sill-like shape of the MTZ gabbro lenses (Fig. 1A) and the presence of graded layers that were thought to indicate a lack of deformation. We have shown that the gabbro lenses are strongly deformed (Fig. 6) and that lenses may have shapes that differ from those of simple sills (Fig. 2H). Also there is no microstructural study showing that the layered gabbro lenses have intrusive contacts, or observations of layered gabbro lenses branching with dikes or any root-like bodies tectonically transposed after emplacement, which would support that the lenses

are the remains of sills. Unlike what can be observed in Oman, Bedard (1990; 1993) describes sharp intrusive contacts, with reaction rims and host rock xenoliths in gabbro sills of the Bay of Island ophiolite. In the Annieopsquotch ophiolite, Lissenberg et al (2004) describe dendritic crystals and comb structures in modally layered gabbro sills, and note that the gabbros do not show any fabric. It is surprising that no such clear symptomatic criteria for a sill origin is present in Oman. This might be because of a lack of compositional or thermal disequilibrium between the lenses and the host rock, but even rare layered sills corresponding to the dying stage of the Oman magmatism are not found. On the contrary, many gabbro lenses have diffuse contacts (Fig. 5) rather than sharp ones, the tip of the lenses often show a progressive transition from the gabbro to the host impregnated dunite over a few centimeters, and all of the layered gabbro have a clear fabric. This suggests that the sill model is not applicable to many of the gabbro lenses of the Oman ophiolite MTZ. Also, the presence of euhedral plagioclase within the impregnated dunite (Fig. 4A) shows that suspension flow is not confined within the lenses, and that the lenses may result from a segregation rather than represent the remains of the melt conduits.

5.2. Melt emplacement.

With its diffuse limits (Fig. 3C), the gabbro of the Khilah outcrop clearly does not represent a sill intrusion. The transition from the impregnated dunite to the gabbro, and the presence of dunite patches within the gabbro strongly suggest that the gabbros represent zones where impregnating melt crystallized great volumes of plagioclase and to a lesser extent clinopyroxene, to the point where the petrologic designation of the rock switches from plagioclase-dunite to troctolite or gabbro although it is in essence a massively impregnated dunite. A consequence of this interpretation is that a part of the olivine grains in the gabbro

must be mantle xenocrysts. The textures, the large grain size (1 to 5 mm), and the coupling of gabbro layers orientation with asthenospheric mantle flow show that melt emplacement at the Khilah outcrop is contemporaneous with mantle flow and thus must be ascribed to ridge processes. This outcrop is structurally above isotropic melt impregnations in depleted harzburgite at the Mahram village, above the Maqsad mantle diapir (Fig. 3). It is beneath a >2 Km wide zone, where gabbros at the base of the crustal section are roughly layered, and resemble those observed at the Khilah outcrop. Isotropic and poorly layered gabbro blocks are particularly abundant in riverbeds near the Khilah outcrop but are also found elsewhere, suggesting that this type of outcrop is not unique. The position at the apex of the mantle diapir, probably centered on the inferred paleoridge axis, may explain why the whole area shows several outcrops that are not strongly affected by the diverging ridge flow. This situation raises the question of how isotropic gabbro bodies evolve when they are not fossilized in this state and endure the deformation imposed by the host rock; the layered gabbro lenses are the only obvious candidates for the possible result.

5.3. Fabric evolution

The poikilitic textures in impregnated dunite show olivine grains that are free to rotate (Fig. 4b), implying that melt reached the critical melt fraction (near 30%, Van der Molen and Paterson, 1979) where the solid matrix is disaggregated by the melt and the fabric is lost, thus forming the type 1 gabbro. Four isotropic CPOs in melt impregnated harzburgite and dunite samples have been reported before (Boudier et al, 1996; Jousselin et al, 1998; Jousselin and Mainprice, 1998), and interpreted in this manner; however in these cases only a small fraction of plagioclase and clinopyroxene was precipitated from the melt in the residual dunite, thus the modal composition was not shifted towards that of a gabbro. The situation observed in the

Khilah outcrop is rare because it shows a stage that can only be ephemeral. As melt progresses through the solid dunitic matrix, it fills more space, thus the fluid pressure will drop, and the melt mush will start to compact. This will lead to fading of the type 1 stage and emergence of a planar fabric which is exactly what is observed in type 2 samples.

As melt fraction decreases and more transient solid chains form and interact, coupling with the simple shear imposed by the surrounding mantle flow is more efficient, and leads to the development of a stronger magmatic lineation in the olivine and plagioclase CPO as seen in type 3 samples. [001] (010) olivine CPO is generated by magmatic flow (Benn and Allard, 1988), or may be favored by plastic deformation in the presence of melt (Holtzmann et al, 2003) or by mantle hydratation (Jung and Karato, 2001). The euhedral shape, the preferred shape orientation and its correlation with the CPO, and the context of the magmatic rock with magmatic texture for plagioclase, where most olivine grains are embedded in plagioclase and clinopyroxene grains that are themselves not deformed, suggest that at this stage plastic intracrystalline deformation is not a major factor to produce the CPO. We interpret the [001](010) olivine CPOs in type 3 as similar to the magmatic fabric in a sample of Oman layered gabbro of the crustal section (Benn and Allard, 1988). Note that the term "magmatic" refers to the physical conditions required to orient crystals without any intracrystalline deformation; it does not refer to the olivine origin which can be cumulative or mantellic. As the [001] axis is the longest axis in euhedral olivine, it aligns with the flow, and the CPO reflects the shape fabric. The [100] (010) plagioclase CPO in type 3 and type 4 samples compare well with previously reported magmatic fabrics (see review in Benn and Allard, 1988), and the lack of evidence for plastic deformation leaves no doubt that the plagioclase fabrics are of magmatic origin.

Type 4 samples show a [100](010) olivine CPO which corresponds to the classic high-temperature gliding system. The unique case of [100] (001) CPO also corresponds to a less common high-temperature gliding system; it has been reported in two harzburgite samples of the Maqsad diapir (unpublished personal data), a harzburgite at the Garret transform (Cannat, et al, 1990), Hess Deep (Boudier et al, 1996b), and dunite associated with chromite pods in the New Caledonia ophiolite (Cassard et al, 1980); i.e. cases where the peridotite is associated with melt circulation. We now try to understand how such a plastic fabric can be generated in gabbros with a prominent magmatic texture. Boudier and Nicolas (1995) have reported [100] (010) olivine CPOs for two strongly deformed gabbro samples; they classify the origin of strain in olivine as questionable. Vernon (2000) notes that solid-state strain in the interstices between undeformed and aligned crystals may assist rotation and alignment without plastic deformation of the rotated crystals. While he considers observations where the solid-state strain is thought to be minor, he also points out that it is unknown to what degree this process can produce strong alignment of undeformed crystals. Indeed, in solid-state deformation, large viscosity contrasts may also be present and mechanisms of particle orientation in magmatic flow can also apply to the situation of rigid crystals embedded in a weak solid matrix deforming plastically, such as amphiboles in a phyllite (Fergusson, 1979). Experimental constraints for plagioclase deformation at high temperature suggest that olivine is weaker than plagioclase at oceanic Moho conditions (Seront, 1993; Dimanov et al, 1998). The possibility of deforming olivine plastically while plagioclase crystals remain undeformed is enhanced by the strong segregation observed at this stage. We argue that as a critical threshold of olivine connectivity is reached, olivine deformation rapidly switches from magmatic to plastic. This last stage of deformation probably contributes to the layering sharpening, as deformation must concentrate in the weakest layer: either melt (and possibly

plagioclase) rich layers if enough melt is present within this layer, or more probably at this last stage, olivine rich layers when the melt fraction is greatly reduced.

Once gabbro is fully crystallized, it must be under lithospheric conditions (i.e. mantle flow is frozen). As no low temperature deformation is recorded, gabbro in lithospheric conditions must simply drift away from the ridge axis and not be further deformed. Thus the strong olivine plastic fabric must develop in a tight window at the asthenosphere/lithosphere boundary, with little or no melt, where most of the deformation is accommodated by the olivine rich layers. This implies that under high temperature conditions, and with the presence of melt to enhance diffusion, simple shear is capable of erasing the pre-existing type 3 fabric and of producing a new and strong plastic olivine CPO, within a few hundred meters of flow.

It is interestingly fitting that the samples with the largest fractions of clinopyroxene are type 3 and type 4 gabbros. For a parental MORB melt, clinopyroxene must be the last phase to crystallize, at near 1160°C (Feig et al, 2006), when the mush is crystal-rich and the final stages of deformation are reached. Still, more data are needed to establish a correlation between modal composition and gabbro types, and we will see in the next section that modal composition should be used with caution.

IODP hole 1309D, at the Mid-Atlantic ridge, traverses melatroctolites, troctolites and olivine gabbros that might be viewed as similar to our samples. In the IODP hole, the olivine CPO is thought to result from a mantle fabric modified by incoming melt, which corroded olivine grain boundaries and penetrated along olivine tilt walls (Drouin et al, 2010). We do not think that the fabrics of our samples are inherited from a previous mantle fabric. The IODP samples show small olivine grains embedded in large plagioclase poikiloblasts; whereas in our

399 samples, olivine crystals remain large, they do not show evidence for corroded boundaries,
400 and the plagioclase blades are not parallel to olivine tilt walls. Our outcrops top the
401 harzburgite section, whereas those of the IODP hole lie above evolved gabbro, which indeed
402 could provide an evolved melt able to dissolve olivine grains (Suhr et al, 2008). Finally, the
403 CPO analysis of the IODP samples relies on the relative concentration of maxima for each
404 crystallographic axis rather than their orientation as no X,Y,Z structural frame nor layering is
405 visible. It shows strong maxima for the [001] axis, which is not something we observe in our
406 samples.
407
408 Given the field relationships, and the coincidence of the different CPOs with aspects of the
409 shape fabric and layering in our samples, we argue that there is a continuum from type 1
410 samples where all mantle fabric heritage is lost, to type 4 samples where a new fabric is
411 produced (Fig. 8). In this last stage, where olivine is so segregated that it constitutes thin
412 dunite-like layers, the fabric is similar to the host dunite fabric to which it is coupled. We
413 suppose that many of the olivine crystals in the gabbro are of mantellic origin, but this is
414 deduced from the texture of type 1 samples, not from the fabric developed in type 3 and type
415 4 samples, which could equally affect olivine of magmatic origin.
416
417 *5.4. Layering formation*
418
419 Most of the observed microstructures imply a strong simple shear deformation. We show that
420 layering does not predate shearing but is linked to the development of deformation. The CPOs
421 induced by the simple shear allow us to follow a continuous evolution of the deformation
422 which is correlated with the development of layering defined by type 1 to type 4 samples.
423 Field relations from type 1 to type 2 and 3 at the Khilah outcrop, and from the type 3 to type 4

in other places are coherent with this evolution, and we think it is unlikely that the different types represent unrelated gabbro bodies. This idea is reinforced by the consideration that types 1 to 3 do not represent steady-state situations, and should be more deformed when they are not frozen at this stage.

Some of the reasons why simple shear in magmatic rocks can cause crystal and melt segregation are summarized by McBirney and Nicolas (1997). At least two processes are relevant to the generation of layering in our case: segregation of suspended solids (crystals) of differing sizes, and transposition of inhomogeneities. Similarly, the creation of layering by shearing is accepted in plastically deformed rocks, where a "massive" (unlayered) plutonic rock can turn into a layered gneiss, with better defined and thinner layers for more strongly deformed rocks (e.g. Myers, 1978). Also, shearing lead to transpose heterogeneities into lenticular beds (e.g. Ramsay and Graham, 1970) producing other layers. In addition there is a wide range of physical experiments and models that produce segregation in suspended particles, slurries, or granular material during simple shear deformation (e.g. Sokolowski and Herrmann, 1992; Santra et al, 1996; Barentin et al, 2004; May et al, 2009), including asymmetric layers (e.g. Komnik et al, 2004). These investigations indicate that any type of difference in the particle species may lead to shear-induced segregation (Plantard et al, 2006). This suggests that the complexity of crystal size, geometry, surface properties, and density variations provide multiple factors favoring the generation of layers. On the basis of these studies and our observations, we argue that a large fraction of gabbro layering can originate from mechanical sorting during strong shearing and tectonic transposition of heterogeneities. This model solves a paradox pointed by Koga et al (2001): the highly variable lithologies are thought to arise via different degrees of crystal fractionation from a common parental melt; however, the limited range of variability in olivine, plagioclase and clinopyroxene

compositions suggests that the differences in extent of crystallization must be small. If layers are created through mechanical sorting, their modal compositions do not reflect crystal fractionation variations from a sequence to another, and it becomes possible to create various lithologies from a single cumulate sequence.

5.5. Timing and consequences on melt extraction process

The small frequency of isotropic or weakly deformed gabbros suggests that they are transient features, which are not often preserved because they must be frozen in the short time lapse between emplacement and the shearing and tectonic transposition inexorably imposed by the surrounding mantle flow. This is coherent with the observation of residual harzburgite in isotropic impregnations, where the orthopyroxene dissolution reaction with incoming melt is started but not completed, whereas transposed melt impregnations imply sufficient time for deformation to accumulate and thus longer melt residence within the rock, leading to resorbtion of all the orthopyroxene grains.

The isotropic stage implies that melt accumulated rapidly with respect to the mantle strain rate. How fast melt accumulates (t) can be estimated by dividing the volume of melt that was present, by the melt flux from the melt feeding conduit. Considering that isotropic gabbro is distributed in a sphere with a diameter L equal to the length of the outcrop, and that the minimum melt fraction corresponds to that required to disaggregate the solid framework (30%), it gives:

$$t = [4/3 \times (L/2)^3 \times 0.3]/[V_m \times (D/2)^2 \times f]$$

where V_m is the ascending melt velocity, D is the diameter of the melt conduit which we take as circular, and f is the melt fraction in this conduit. For a porous flow melt conduit, values on

the order of one meter per year for V_m, one hundred meters for D, and one percent for f seem reasonable (Kelemen et al, 1997b). This gives a time of 250 000 years. On the other hand, gabbro layering seems to develop over distances less than a hundred meters as type 2 and 3 samples are present within the Khilah outcrop and at its outskirts. Given that the host dunite flows at a velocity near the ridge spreading velocity or faster (Jousselin et al, 1998), for a velocity around 10 cm/year we conclude that layering must develop over a time of about a thousand years.

These numbers are not very precise, and are only intended to provide orders of magnitude. There was probably more than 30% melt present at the time of the formation of the Khilah outcrop, mantle foliation geometry and shear sense inversion beneath the Moho suggest that mantle flow is faster than ridge spreading rate (Ildefonse et al, 1995, Michibayashi et al, 2000), and dunite bands that are interpreted as relics of porous flow conduits, are often thinner than a hundred meters. So the discrepancy between the two results could be more important. This suggests that porous flow conduits cannot deliver melt fast enough to destroy the solid framework of the host dunite and accumulate within a time window small enough to not be affected by the host rock shearing. Another possibility is that melt was extracted from dikes, as proposed by Nicolas (1986) for depth of 0 to 60 Km, and by Kelemen et al (1997b) for very shallow mantle. It would take less than a year and a half for a 10 cm wide and 100 m long dike, with a melt velocity of 1.5 cm/s (Lago et al, 1982) to fill the necessary melt volume.

5.6. Origin of gabbro layering in the lower crust?

We investigate whether our model for the origin of layering in gabbro lenses of the MTZ is adaptable to gabbro layers in the lower crust. Several lines of evidence suggest that this is possible: recent marine geophysical investigation shows that the lower gabbros contain similar local melt accumulations (Canales et al, 2009); Nicolas (1992) indicates that the strong simple shear kinematic criteria are also ubiquitous in the layered gabbros of the crustal section; we found type 2 and type 3 crustal gabbro at the inferred Maqsad paleoridge axis, and out of the 3 published olivine CPOs measured in crustal layered gabbro, one presents a [001](010) fabric, typical of the type 3 gabbro (Benn and Allard, 1988). As the host rock is not dunite, it is possible that the gabbro is devoid of olivine xenocrysts, and that melt recycles plagioclase and clinopyroxene crystals of the host rock instead. On the other hand, wehrlite crustal intrusions, which are rooted in the MTZ magmatic mush, may provide an olivine xenocryst source, and may produce olivine rich layers when they are tectonically transposed into concordance by the surrounding magmatic flow (Jousselin and Nicolas, 2000; Koga et al, 2001).

6. Conclusion

We show that modal layering in gabbro lenses of the MTZ does not predate shearing but is linked to the development of simple shear deformation, imposed by the surrounding mantle flow. We collected the first extensive CPO dataset for these rocks, which allows us to follow the coevolution of deformation and layering. We found three distinct deformation stages that follow the emplacement of isotropic gabbro. First the melt mush is compacted, leading to planar fabric (type 2 gabbros) and the emergence of a rough layering. Then simple shear leads to a magmatic (driven by the shape of crystals in suspension) fabric (type 3 gabbros); at this stage layer boundaries are very irregular and layer extension is limited to a couple meters at

the most. In the last stage (type 4 gabbros), segregated olivine bands switch to high-temperature plastic fabrics, layer boundaries are very sharp and often can be followed over more than three meters. Most gabbro layers are fossilized at this last stage. To fossilize the initial isotropic stage, the melt input must be fast relative to the host dunite strain rate. This suggests that melt reached the MTZ through hydrofracturing dikes. When melt ceases to rise and ponds at the Moho level, textural analysis shows that it disperses through the host dunite and isolates olivine grains; as a result, a large fraction of the olivine grains in the layered gabbro lenses of the MTZ must be mantle xenocrysts.

The sheeted sill model for the Oman ophiolite gabbros mainly relies on the observation of isolated layered gabbro lenses embedded in mantle dunite, which could not possibly derive from the subsidence of a perched magma lens in the upper crust, and chemical constraints that imply that few layers represent isolated systems (sills or small convection cells within a magma chamber) (Browning, 1984, Kelemen et al, 1997a). On the other hand, gabbro glacier models mainly focus on the identification of strong deformation in layered gabbros of the lower crust. In this model, the deformation is related to the flow out of the magma lens perched at the top of the crustal section, which was the only known magma lens at the time these models were developed. A strong merit of our model is to be coherent with constraints from the sheeted sill and the gabbro glacier models. Our model is not intended to describe the dynamics of the whole magma chamber, but offers an explanation based on new data for the formation of the gabbro layering at the base of the ridge magmatic system.

Acknowledgments

This work was supported by the BQR program of INPL-Nancy Université. The authors are grateful to Cédric Demeurie (Fr Eau-Sol-Terre) and Christophe Nevado (Géosciences Montpellier) for the high-quality polished thin sections, David Mainprice for the use of his softwares to plot pole figures, Andréa Tommasi for facilitating the access to the electron microscopy facilities at Géosciences Montpellier, and the Directory of Minerals at the Ministry of Commerce and Industry of the Sultanate of Oman for their hospitality. We also wish to thank George Ceuleneer and an anonymous reviewer for helpful comments.

References

Barentin, C., Azanza, E., Pouligny, B., 2004, Flow and segregation in sheared granular slurries, Europhys. Lett., 66, 139 doi: 10.1209/epl/i2003-10191-2

Bédard, J.H., 1990, Cumulate recycling and crustal evolution in the Bay of Island ophiolite, J. Geol., 99, 225– 249.

Bédard, J.H., 1993, Oceanic crust as a reactive filter: synkinematic intrusion, hybridization, and assimilation in an ophiolitic magma chamber, western Newfoundland, Geology, 21, 77–80.

Benn, K., Allard, B., 1988, Preferred mineral orientations related to magmatic flow in ophiolite layered gabbros, Journal of Petrology, 30, 925-946, doi: 10.1093/petrology/30.4.925.

Ben Ismaïl, W., Mainprice, D., 1998, An olivine fabric database: an overview of upper mantle fabrics and seismic anisotropy, Tectonophysics, 206, 145-157, doi:10.1016/S0040-1951(98)00141-3.

571 Boudier, F., 1991, Olivine xenocrysts in picritic magmas, an experimental and microstructural
572 study, Contributions to Mineralogy and Petrology, 109, 114-123, doi: 10.1007/BF00687204.
573 Boudier, F., Nicolas, A., 1995, Nature of the Moho transition zone in the Oman ophiolite,
574 Journal of Petrology, 36, 777-796, doi:10.1093/petrology/36.3.777.
575 Boudier, F., Nicolas, A., Ildefonse, B., 1996a, Magma chambers in the Oman ophiolite: fed
576 from the top and the bottom, Earth and Planetary Science Letters, 144, 239-250,
577 doi:10.1016/0012-821X(96)00167-7.
578 Boudier, F., MacLeod, C.J., and Bolou, L., 1996b, Structures in peridotites from site 895,
579 Hess Deep: implications for the geometry of mantle flow beneath the East Pacific Rise, In
580 Mével, C., Gillis, K.M., Allan, J.F., and Meyer, P.S. (Eds.), Proc. ODP, Sci. Results, 147:
581 College Station, TX (Ocean Drilling Program), 347–356.
582 Boudier, F., Nicolas, A., Ildefonse B., Jousselin, D., 1997, EPR microplates, a model for the
583 Oman ophiolite, Terra Nova, 9, 79-82, doi: 10.1111/j.1365-3121.1997.tb00007.x.
584 Browning, P., 1984, Cryptic variations within the cumulate sequence of the Oman ophiolite:
585 Magma chamber depth and petrological implications, Geol. Soc. London Spec. Publ. 13, 71–
586 82.
587 Canales, J.P., Nedimovic, M.R., Kent, G., Carbotte, S.M., Detrick, R., 2009, Seismic
588 reflection images of a near-axis melt sill within the lower crust at the Juan de Fuca ridge,
589 Nature, 460, 89-93, doi: 10.1038/nature08095.
590 Cannat, M., Bideau, D., Hébert, R., 1990, Plastic deformation and magmatic impregnation in
591 serpentinized ultramafic rocks from the Garrett transform fault (East Pacific Rise), Earth and
592 Planetary Science Letters, 101, 216-232, doi:10.1016/0012-821X(90)90155-Q.
593 Caress, D.W., Burnett, M.S., Orcutt, J.A., 1992, Tomographic image of the axial low-velocity
594 zone at 12°50'N on the East Pacific Rise, Journal of Geophysical Research, 97, 9243-9263,
595 doi: 10.1029/92JB00287.

596 Cassard, D., 1980, Structure et origine des gisements de chromite du massif du Sud (ophiolite
597 de Nouvelle Calédonie). Guides de prospection, These de 3ème cycle, Univ. Nantes, Nantes.
598 Ceuleneer, G., Nicolas, A., Boudier, F., 1988, Mantle flow patterns at an oceanic spreading
599 center: the Oman ophiolite record, Tectonophysics, 151, 1-16, doi:10.1016/0040-
600 1951(88)90238-7.
601 Crawford W., Webb, S.C., 2002, Variations in the distribution of magma in the lower crust
602 and at the Moho beneath the East Pacific Rise at 9°-10°N, Earth and Planetary Science
603 Letters, 203, 117-130, doi:10.1016/S0012-821X(02)00831-2.
604 Detrick, R.S., Buhl, P., Vera, E., Mutter, J., Orcutt, J., Madsen, J., Brocher, T., 1987, Multi-
605 channel seismic imaging of a crustal magma chamber along the East Pacific Rise, Nature,
606 326, 35-41, doi:10.1038/326035a0.
607 Dijkstra A.H., Drury, M.R., Frijhoff R., 2002, Microstructures and lattice fabrics in the Hilti
608 mantle section (Oman Ophiolite): Evidence for shear localization and melt weakening in the
609 crust–mantle transition zone?, Journal of Geophysical Research, 107, 2270,
610 doi:10.1029/2001JB000458
611 Dimanov, A., Dresen, G., Wirth, R., 1998, High-temperature creep of partially molten
612 plagioclase aggregates, Journal of Geophysical Research, 103, 9651-9664,
613 doi:10.1029/97JB03742.
614 Fergusson, C., 1979, Rotations of elongate rigid particles in slow non-newtonian flows,
615 Tectonophysics, 60, 247-262, doi:10.1016/0040-1951(79)90162-8.
616 Drouin, M., Ildefonse B., Godard M., 2010, A microstructural imprint of melt impregnation in
617 slow spreading lithosphere: Olivine- rich troctolites from the Atlantis Massif, Mid- Atlantic
618 Ridge, 30°N, IODP Hole U1309D, Geochem. Geophys. Geosyst., 11, Q06003,
619 doi:10.1029/2009GC002995

620 Garmany, J., 1989, Acumulations of melt at the base of young oceanic crust, Nature, 340,
621 628-632, doi:10.1038/340628a0.
622 Godard M., Jousselin, D., Bodinier, J.L., 2000, Relationships between geochemistry and
623 structure beneath a paleo-spreading centre: a case study of the mantle section in the Oman
624 ophiolite, Earth and Planetary Science Letters, 180, 133-148, doi:10.1016/S0012-
625 821X(00)00149-7.
626 Henstock T.J., Woods, A.W., White, R.S., 1993, the accretion of oceanic crystal by episodic
627 sill intrusion, Journal of Geophysical Research, 98, 4143-4161, doi:10.1029/92JB02661.
628 Higgins, M., 1991. The origin of laminated and massive anorthosite, Sept iles layered
629 intrusion, Quebec, Canada. Contr. Miner. Petrol. 106, 340-54.
630 Holtzman, B.K., Kohlstedt, D.L., Zimmerman, M.E., Heidelbach, F., Hiraga, T. and J.
631 Hustoft, 2003, Melt segregation and strain partitioning: implications for seismic anisotropy
632 and mantle flow. Science, 301, 1227-1230, doi: 10.1126/science.1087132.
633 Ildefonse, B., billau, S., and Nicolas, A., A detailed study of mantle flow away from diapirs in
634 the Oman ophiolite, 1995, in R.L.M. Vissers and A. Nicolas (eds), Mantle and lower crust
635 exposed in oceanic ridges and in ophiolites, Kluwer Academic Publishers, Dordrecht, 163-
636 177.
637 Jousselin, D., Nicolas, A., Boudier, F., 1998, Detailed mapping of a mantle diapir below a
638 paleo-spreading center in the Oman ophiolite, Journal of Geophysical Research, 103, 18153-
639 18170, doi:10.1029/98JB01493.
640 Jousselin, D., Mainprice D., 1998, Melt topology and seismic anisotropy in the mantle
641 peridotites of the Oman ophiolite, Earth and Planetary Science Letters, 164, 553-568,
642 doi:10.1016/S0012-821X(98)00235-0.

643 Jousselin, D., Nicolas, A., 2000, The Moho transition zone in the Oman ophiolite-relation
644 with wehrlites in the crust and dunites in the mantle, Marine Geophysical Researches, 21,
645 229-241, doi: 10.1023/A:1026733019682.
646 Jung, H., and S. Karato, 2001. Water-induced fabric transition in olivine, Science, 293, 1460–
647 1463, doi: 10.1126/science.1062235.
648 Karson, J.A., Collins, J.A., Casey J., 1984, Geologic and seismic velocity structure of the
649 crust/mantle transition in the Bay of Islands ophiolite complex, Journal of Geophysical
650 Research, 89, 6126–6138, doi:10.1029/JB089iB07p06126.
651 Kelemen, P.B., Koga, Shimizu, N., 1997a, Geochemistry of gabbro sills in the crust–mantle
652 transition zone of the Oman ophiolite: implications for the origin of the oceanic lower crust,
653 Earth and Planetary Science Letters, 146, 475–488, doi:10.1016/S0012-821X(96)00235-X.
654 Kelemen P.B., Hirth G., Shimizu N., Spiegelman M., Dick H.J.B., 1997b, A review of melt
655 migration processes in the adiabatically upwelling mantle beneath oceanic spreading ridges,
656 Phil. Trans. R. Soc. Lond. A, 355(1723), 283-318 doi 10.1098/rsta.1997.0010.
657 Koga, K.T., Kelemen, P.B., Shimizu, N., 2001, Petrogenesis of the crust-mantle transition
658 zone and the origin of lower crustal wehrlite in the Oman ophiolite, Geochemistry-
659 Geophysics-Geosystems, 2, 1038, doi:10.1029/2000GC000132.
660 Komnik, A., Harting, J., Herrmann, H.J., 2004, Transport phenomena and structuring in shear
661 flow of suspensions near solid walls, Journal of statistical mechanics: theory and experiment,
662 doi: 10.1088/1742-5468/2004/12/P12003.
663 Korenaga J., Kelemen, P.B., 1997, Origin of gabbro sills in the Moho transition zone of the
664 Oman ophiolite: Implications for magma transport in the oceanic lower crust, Journal of
665 Geophysical Research, 102, 27,729-27,749, doi:10.1029/97JB02604.
666 Lago, B., Rabinowicz, M., Nicolas, A., 1982, Podiform chromite ore bodies: a genetic model.
667 Journal of Petrology, 23, 103–125, doi:10.1093/petrology/23.1.103.

668 Lissenberg, C.J., Bédard, J.H., van Staal, C.R., 2004, The structure and geochemistry of the
669 gabbro zone of the Annieopsquotch ophiolite, Newfoundland: Implications for lower crustal
670 accretion at spreading ridges, Earth and Planetary Science Letters, 229, 105-123,
671 doi:10.1016/j.epsl.2004.10.029.
672 May, L.B.H., Golick, L.A., Phillips, K.C., Shearer, M., K.E. Daniels, 2009, Shear-driven size
673 segregation of granular materials: modeling and experiment, Physical Review E, 81-5 pt 1, p.
674 051301.
675 McBirney, A.R., Nicolas, A.,1997, The Skaergaard layered series. Part II. Magmatic flow and
676 dynamic layering, Journal of petrology, 38, 569-580, doi:10.1093/petroj/38.5.569.
677 Michibayashi, K., Gerbert-Gaillard, L. and Nicolas, A., 2000, Shear sense inversion in the
678 Hilti mantle section (Oman ophiolite) and active mantle uprise, Marine Geophysical
679 Research, 21, 3-4, 259-268, doi: 10.1023/A:1026713909204.
680 Morales, F. G., F. Boudier, A. Nicolas, 2011, Dynamics of melt lens and subsidence of axial
681 magma chamber, Tectonics, 30, TC2011, doi:10.1029/2010TC002697.
682 Myers, J., 1978, Formation of banded gneisses by deformation of igneous rocks, Precambrian
683 Research, 6, 43-64, doi:10.1016/0301-9268(78)90054-2.
684 Nedimovic, M., Carbotte, S., Harding, A., Detrick, R., Canales, J.P., Diebold, J., Kent, G.,
685 Tisher, M., J. Babcock, 2005, Frozen magma lenses below the oceanic crust, Nature, 436,
686 1149-1152.
687 Nicolas, A. Prinzhofer, A., 1983, Cumulative or residual origin for the transition zone in
688 ophiolites: Structural evidence, Journal of petrology, 24, 188–206,
689 doi:10.1093/petrology/24.2.188.
690 Nicolas, A., 1986, A melt extraction model based on structural studies in mantle peridotites,
691 Journal of petrology, 27, 999–1022, doi:10.1093/petrology/27.4.999.

692 Nicolas, A., Reuber, I., Benn, K., 1988, A new magma chamber model based on structural
693 studies in the Oman ophiolite, Tectonophysics, 151, 87-105, doi:10.1016/0040-
694 1951(88)90242-9.
695 Nicolas, A., 1992, Kinematics in magmatic rocks with special reference , to gabbros. Journal
696 of Petrology 33, 891–915, doi:10.1093/petrology/33.4.891.
697 Nicolas, A., Boudier, F., Ildefonse, B., 1996, Variable crustal thickness in the Oman ophiolite,
698 implication for oceanic crust, Journal of Geophysical Research, 101, 17,941-17,950,
699 doi:10.1029/96JB00195.
700 Plantard, G., Saadaoui, H., Snabre, P., Pouligny, B., 2006, Surface-roughness-driven
701 segregation in a granular slurry under shear, Europhys. Lett., 75(2), 335-341, doi:
702 10.1209/epl/12006-10088-6.
703 Quick, J.E., Denlinger, R.P., 1993, Ductile deformation and the origin of layered gabbro in
704 ophiolites, Journal of Geophysical Research, 98, 14015-14027, doi:10.1029/93JB00698.
705 Ramsay,J.G., Graham, R.H., 1970, Strain variation in shear belt, Can. J. Earth Sci., 7, 786-
706 813, doi: 10.1139/e70-078.
707 Rabinowicz M., Ceuleneer G., Nicolas A., 1987, Melt segregation and asthenospheric flow in
708 diapirs below spreading centers: evidence from the Oman ophiolite. Journal of Geophysical
709 Research, 92, 3475-3486, doi:10.1029/JB092iB05p03475.
710 Sano S., Kimura, J.-I., 2007, Clinopyroxene REE geochemestry of the Red Hills peridotites,
711 New Zealand: interpretation of magmatic processes in the upper mantle and in the Moho
712 transition zone, Journal of petrology, 48, 113-139, doi:10.1093/petrology/egl056.
713 Santra, S.B., Schwarzer, S., Hermann, H., 1996, Fluid-induced particle size segregation in
714 sheared granular assemblies, Physical Review E., 54, 5, 5066-5072.
715 Serront, 1993, Déformation expérimentale à haute pression et haute température d'aggrégats
716 polycristallins de plagioclase et d'olivine. Thèse de Doctorat, Montpellier, 237p.

717 Sinton, J.M., 1977, Equilibration history of the basal alpine-type peridotite, Red Mountains,
718 New Zealand, Journal of petrology, 18, 216-246, doi:10.1093/petrology/18.2.216.
719 Smewing, J.D., 1981, Mixing characteristics and compositional differences in mantle-derived
720 melts beneath spreading axes: evidences from cyclically layered rocks in the ophiolite of
721 North Oman, Journal of Geophysical Research, 86, 2645-2659,
722 doi:10.1029/JB086iB04p02645.
723 Sokolowski S., Herrmann, H.J., 1992, Dynamic phase separation of a fluid mixture,
724 Europhysics Letters, 18, 5, 415-420.
725 Suhr, G., E. Hellebrand, K. Johnson, Brunelli D., 2008, Stacked gabbro units and intervening
726 mantle: A detailed look at a section of IODP Leg 305, Hole U1309D, Geochem. Geophys.
727 Geosyst., 9, Q10007, doi:10.1029/2008GC002012
728 Molen, I. Paterson, M.S., 1979, Experimental deformation of partially-melted granite.
729 Contributions to Mineralogy and Petrology, 70, 299-318, doi: 10.1007/BF00375359.
730 Vernon, R.H., 2000, Review of microstructural evidence of magmatic and solid-state flow,
731 Electronic Geosciences, 5:2, doi: 10.1007/s10069-000-0002-3.
732 Yaouancq, G., MacLeod, C.J., 2000, Petrofabric investigation of gabbros from the Oman
733 ophiolite: comparison between AMS and rock fabric, Marine Geophysical Researches, 21,
734 289-305, doi: 10.1023/A:1026774111021.
735
736
737 **Tab and figure caption**
738
739 Table 1: Modal composition at the thin section scale for a selection of our samples. See the
740 microstructural analysis paragraph for the definition of gabbro type. Modal composition
741 within different layers is provided when layer boundaries are observed within the thin section.

Figure 1: 3 views on layered gabbro lenses at outcrop/sample/thin section scales. A) A series of 10-40 cm thick layered gabbro lenses embedded in dunite. Hammer handle is 40 cm. B) Close up views on layers within a lens, with sharp and linear boundaries (referred as type 4 in the text). Pictures height is 30 cm. C) Thin section phase maps of samples 07OD48 (top) and 07OD47B3 (bottom) constructed from MEB-EBSD measurements (N.I.: not indexed).

Figure 2: views on isotropic, poorly layered, and irregular-shaped gabbro layers and patches. A) Isotropic gabbro at the center of the Khilah outcrop. B) Dunitic small bodies with random orientations and diffuse contacts within isotropic gabbro at the Khilah outcrop. C-D) Two examples of 1 m-long rough layers emerging from isotropic gabbro (referred as type 2 in the text). E-F) slightly better developed layering, with wavy boundaries and frequent layer terminations (referred as type 3 in the text) G) Several discordant layers H) small altered gabbroic lens with an irregular shape, with its longest axis approximately parallel to the stretching lineation in host dunite.

Figure 3: A) Lineation map of the Maqsad diapir (adapted from Jousselin et al, 1998) with samples distribution. B) close up on the situation of the Khilah outcrop; location shown by a rectangle in A. The Khilah outcrop is the southernmost and largest circled isotropic gabbro outcrop. C) Boulders collected at the Khilah outcrop, with progressive increase in plagioclase and clinopyroxene content, mimicking the diffuse transition from impregnated dunite to gabbro. D) Field sketch of the eastern part of the Khilah outcrop; location shown by a grey rectangle in B); the western part is more monotonous with essentially isotropic gabbro.

Figure 4: close up on melt impregnated dunite at the periphery of the Khilah outcrop. A) plagioclase and clinopyroxene impregnated dunite in the MTZ near the Mahram pass (see Fig. 3B), with a few automorphic plagioclase grains (pointed by arrows). B) plagioclase oikocrysts isolating olivine grains in the impregnated dunite at the western limit of the Khilah outcrop.

Figure 5: from bottom to top, (1) foliated plagioclase impregnations in dunite, (2) three 1 cm bands, rich in plagioclase aggregates of impregnating crystals, and (3) thin lenses of layered gabbro (type 4) in the background.

Figure 6: kinematic indicators of simple shear in layered gabbro lenses. A-B) Asymmetrical folds; as is the case for strong deformation, fold axis are rotated parallel to the lineation direction. C-D) Normal shear zones in cross-section and planar view. The planar view shows the consistent orientation of the shear plane, and the cross-section view explains the color variations in map view induced by the movement at the shear zone. E) Close-up view on a layer with olivine crystals at a consistent angle to the layering.

Figure 7: a selection of fabrics and shape fabrics from our microstructural study. A) Olivine CPO for a dunite (host rock of the gabbro lenses) showing a classic [100] (010) mantle fabric. The obliquity between the [100] axis and the lineation [X] indicates a dextral shear sense. B) Histograms of the orientation of the long axis in XZ thin sections of plagioclase grains for four samples. The lineation corresponds to the 90° orientation. As deformation progress from type 1 to type 4 gabbros, measurements show a better shape preferred orientation parallel to the lineation. C) CPO of olivine and plagioclase for 6 samples, showing deformation evolution in the 4 sample types. Type 1 samples show no CPO; type 2 samples show a planar fabric defined by the (010) planes of olivine and plagioclase; type 3 samples show a [001]

(010) olivine and [100] (010) plagioclase magmatic fabric, with a lineation superimposed on the planar fabric. Type 4 gabbros are characterized by a switch to olivine plastic deformation with a strong [100] lineation. Contours are at 0.5% intervals of uniform distribution.

Figure 8: model for the formation of layered gabbro lenses. The model relies on the correlations of gabbro lenses shape changes, the absence of layering in type 1 gabbro and the development of layering from type 2 to type 4 gabbros, and the evolution of the fabric due to the host mantle (gray) shearing; it implies melt (white) delivery from dikes, and integration of mantle olivine within layered gabbros

Melt impregnation forms isotropic gabbro in the Oman ophiolite Moho transition zone

We measured crystallographic fabric for transition from isotropic to layered gabbro

Olivine fabric evolves from planar to [001](010)-magmatic to [100](010)-HTplastic

We deduce that gabbro layering originates from shear caused by host mantle flow

Isotropic stage means melt collected faster than shear rate, thus extracted by dikes

Graphical Abstract

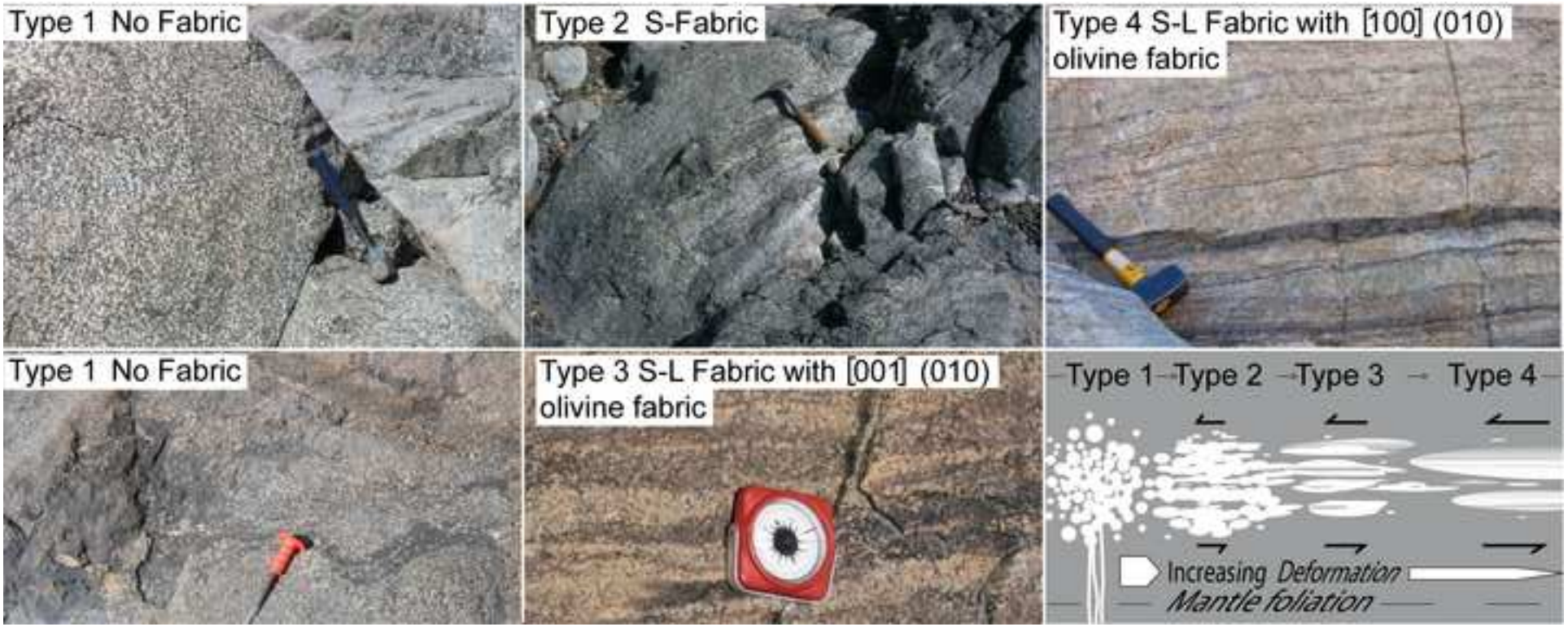

Figure 1

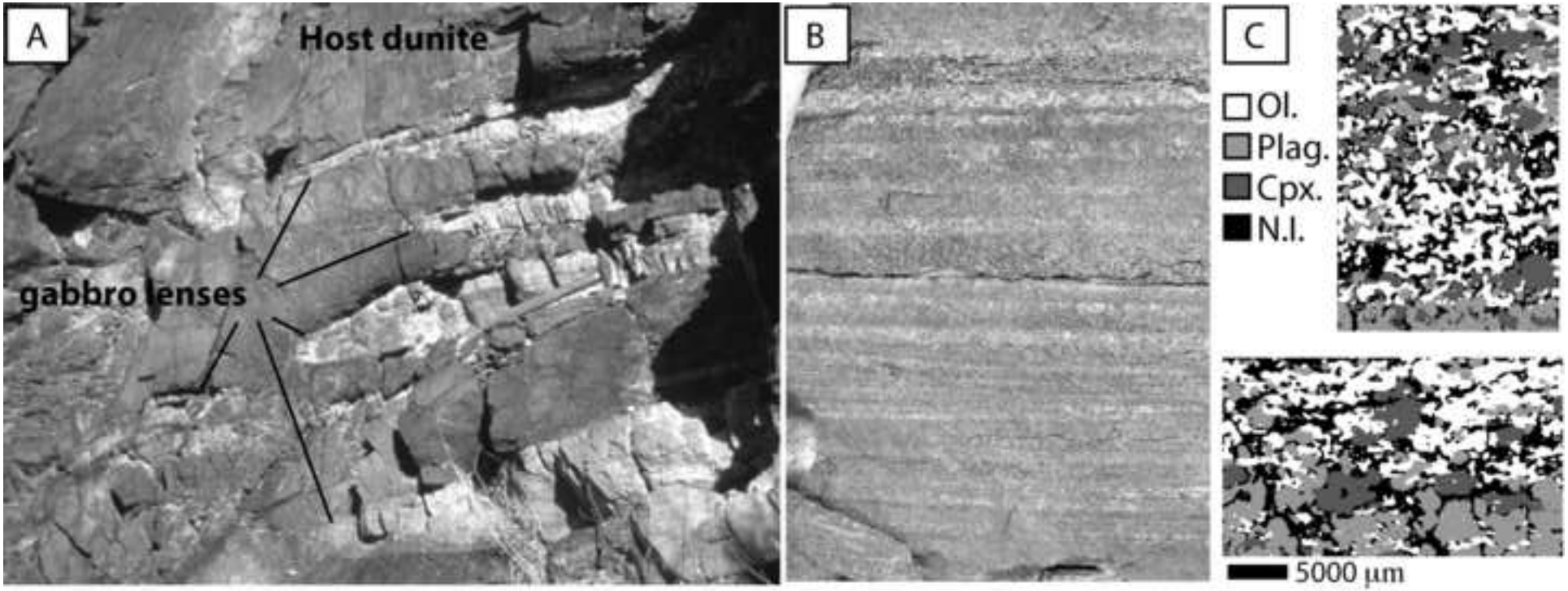

Figure 1 colour version (online only, not readable printed B&W)

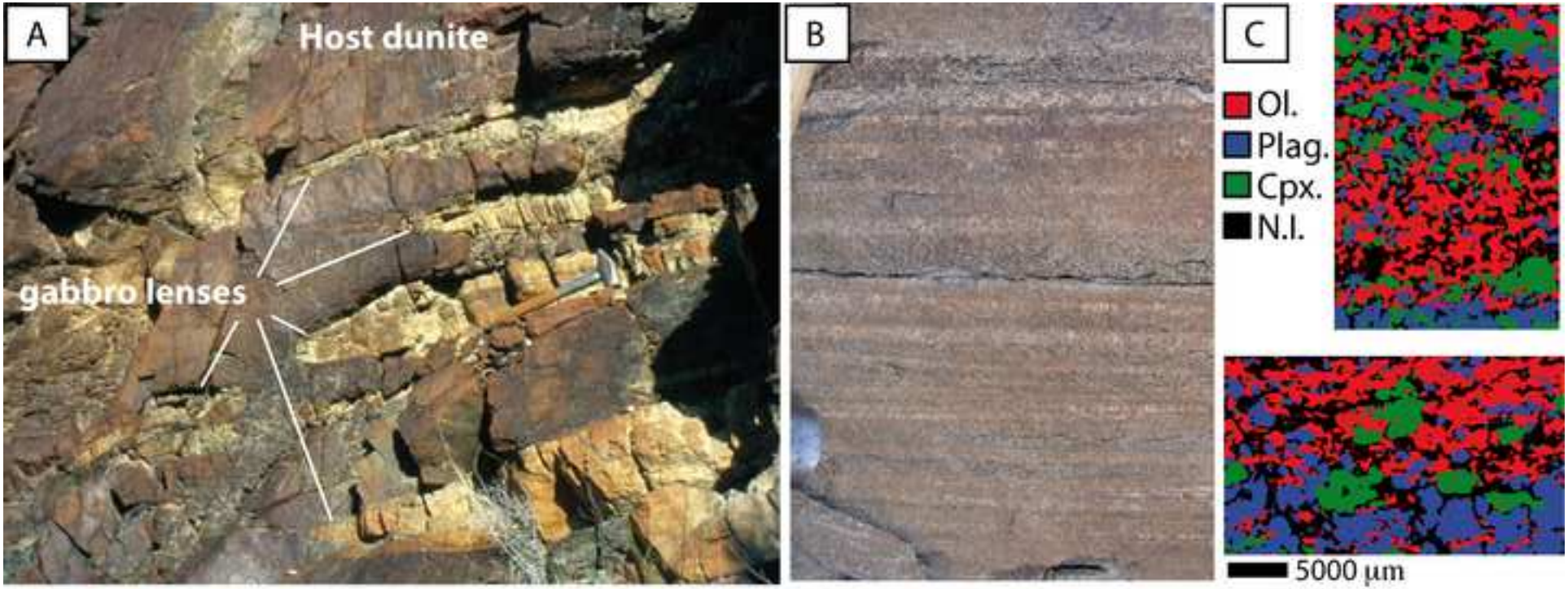

Figure 2 (can be printed in B&W)

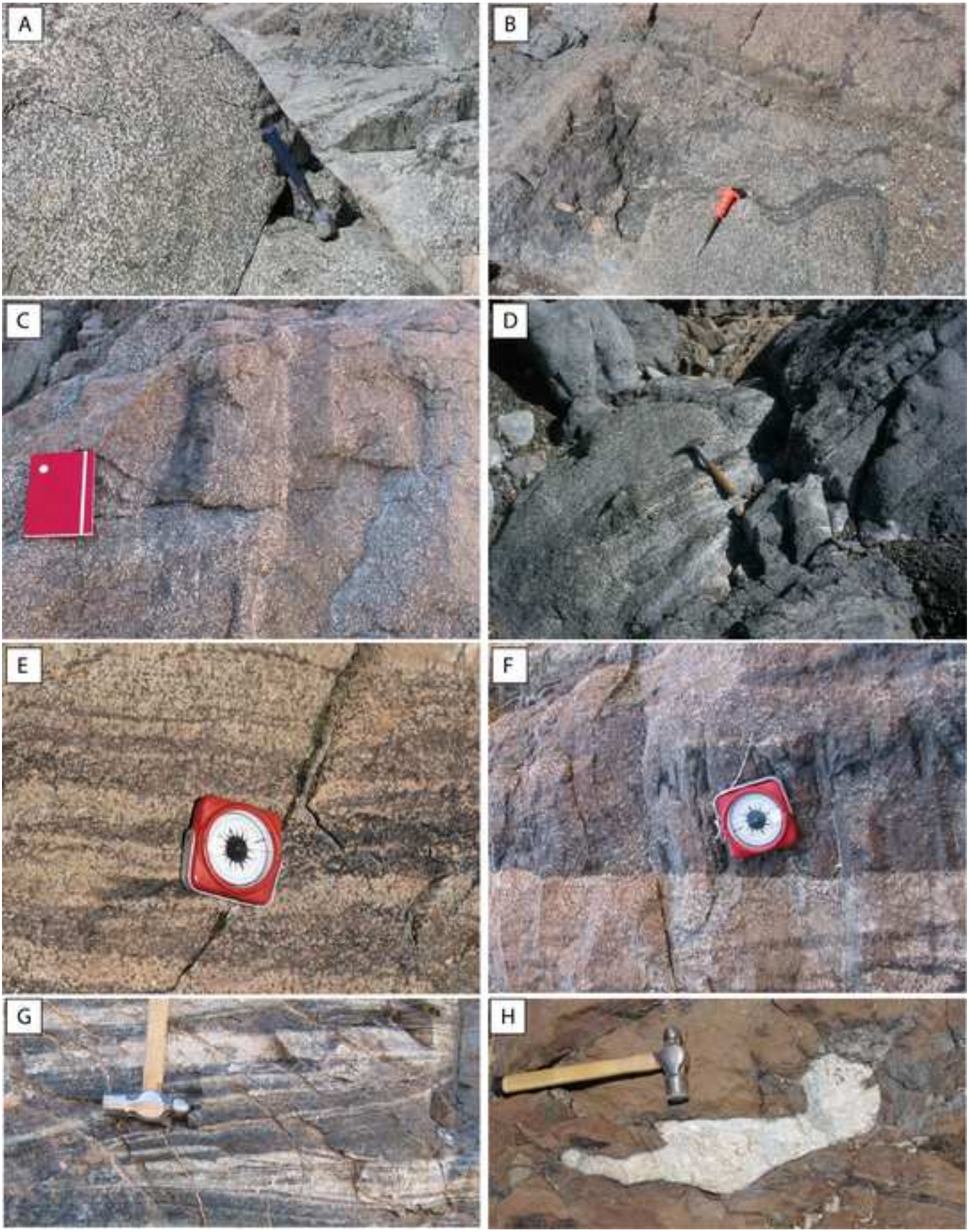

Figure 3 (can be printed in B&W)

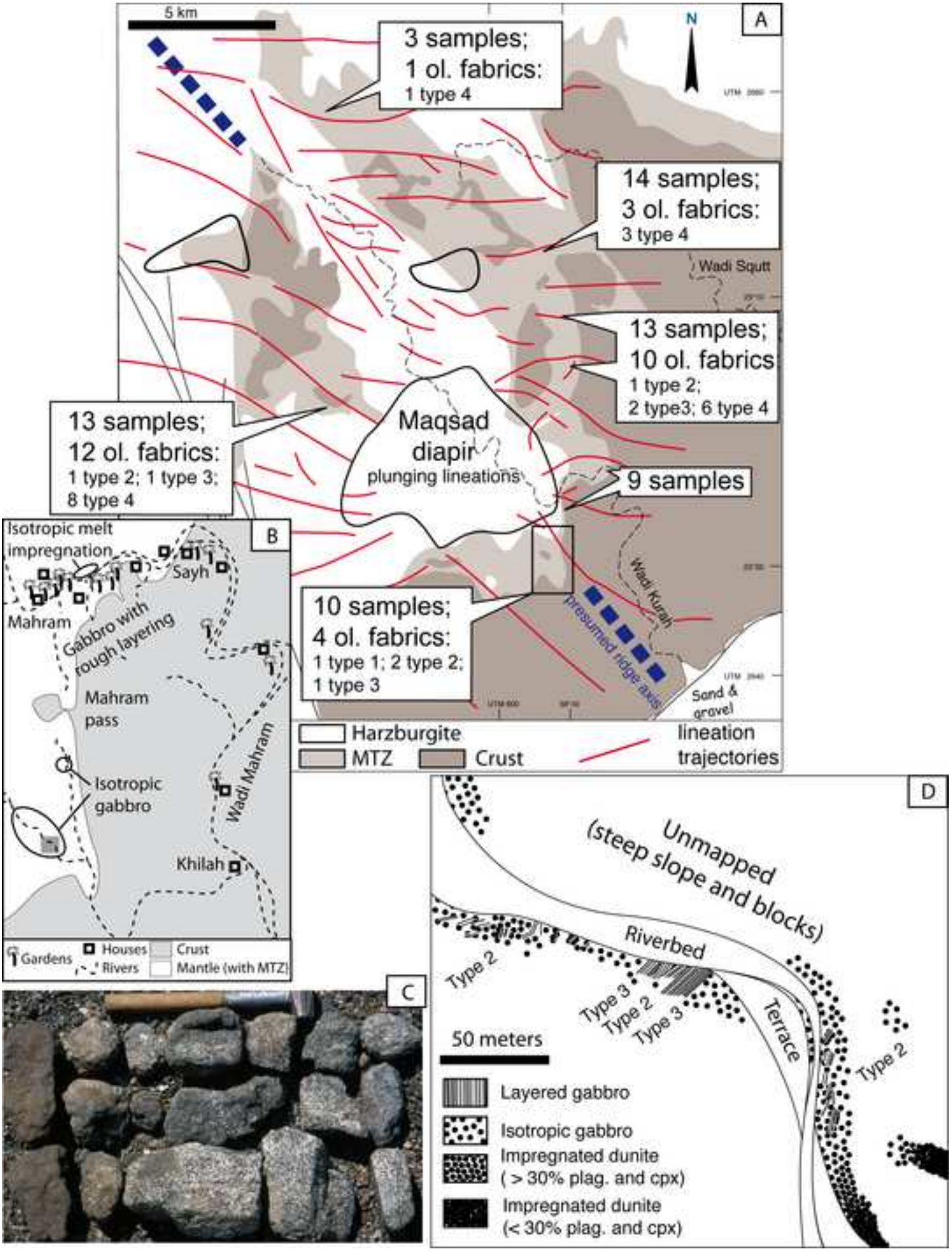

Figure 4 (can be printed in B&W)

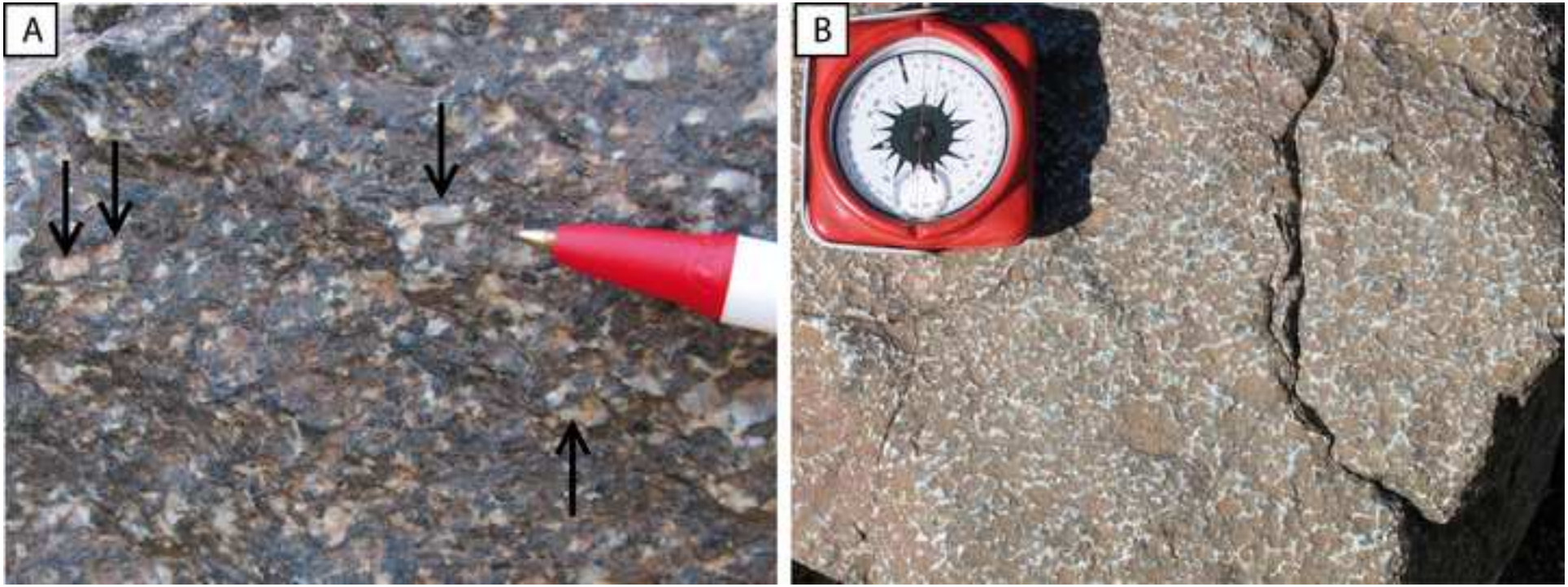

Figure 5 (can be printed in B&W)

Figure 6 (can be printed in B&W)

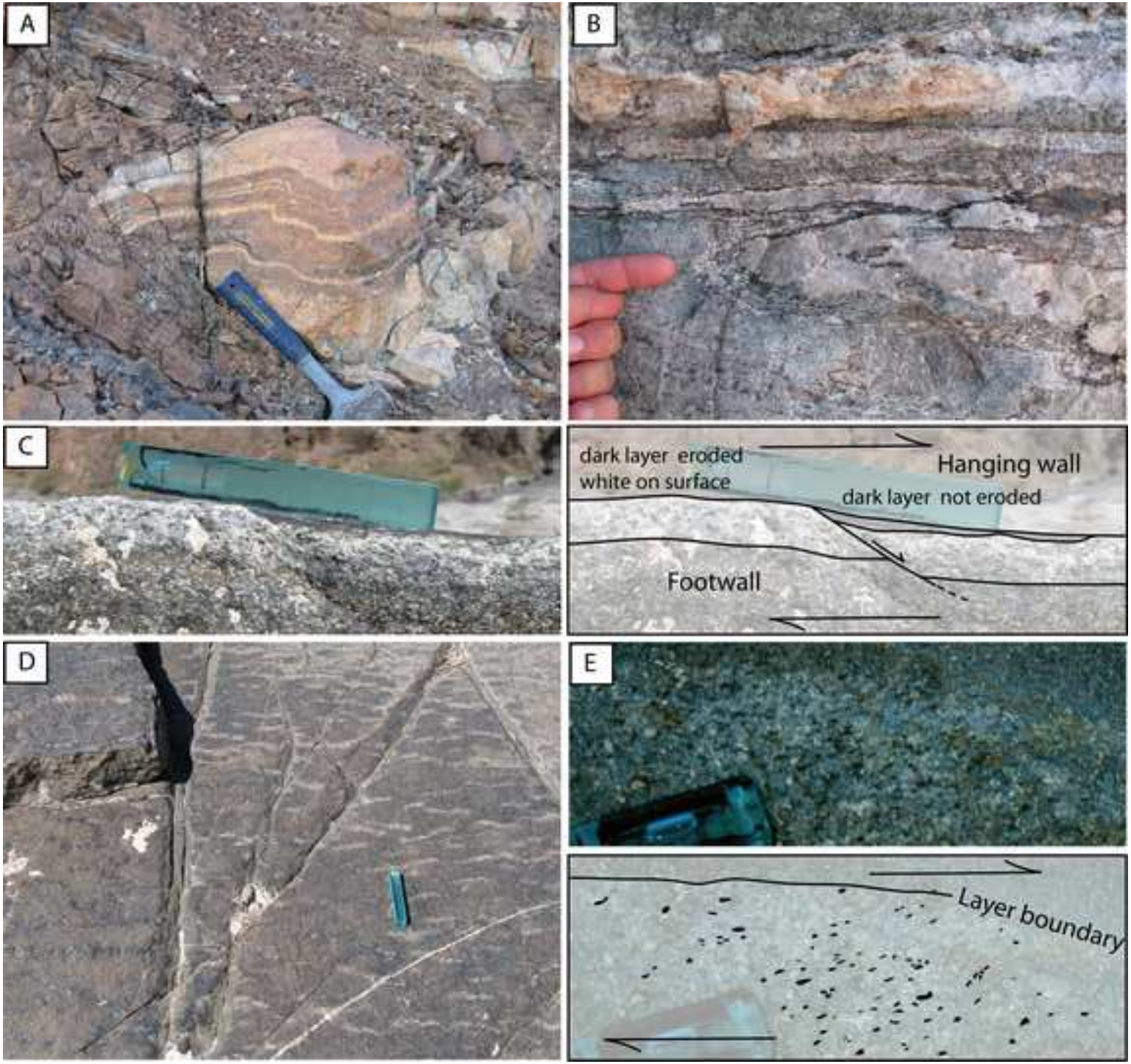

Figure 7 (can be printed in B&W)

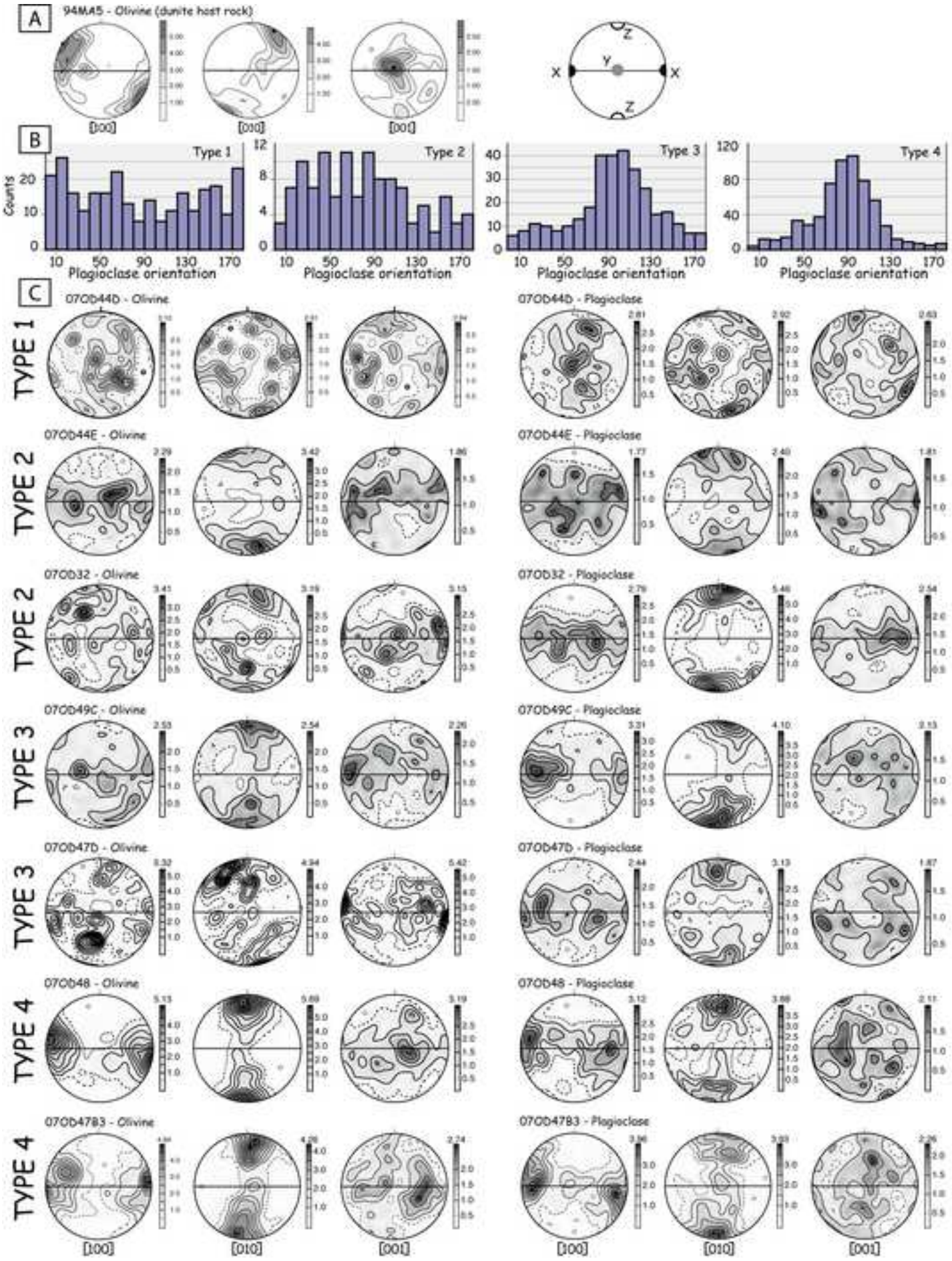

Figure 8 (can be printed in B&W)

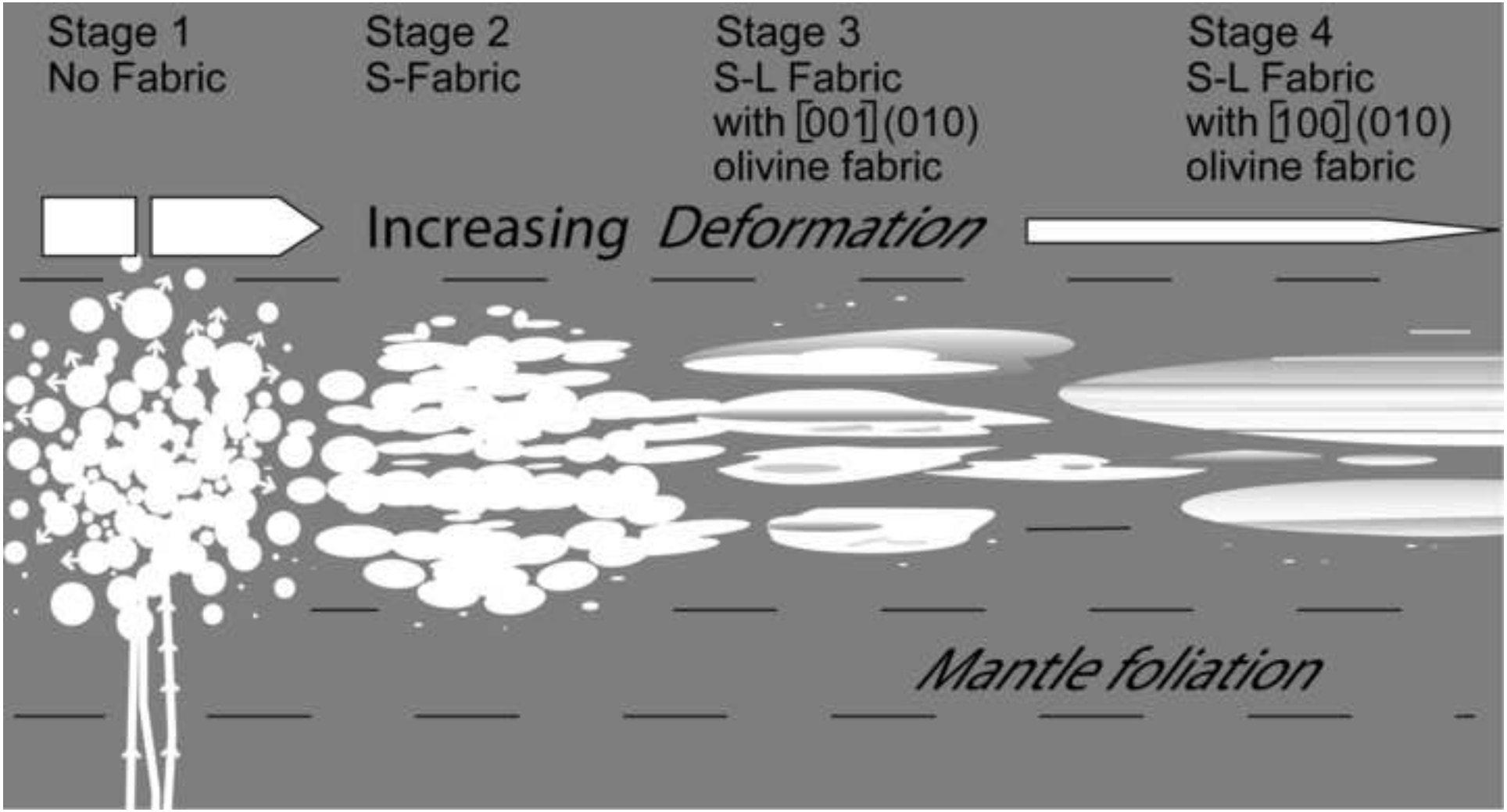

Table

Sample/ layers	Type	Modal composition **Global**/layer ol-plag-cpx	
07OD44D unlayered	1	**15-75-10**	
07OD49E unlayered	1	**22-78-0**	
07OD44B 1 layer	2	**15-76-9**	
07OD44E 1 layer	2	**14-89-1**	
07OD21B 1 layer	2	**19-77-4**	
07OD32 2 layers	2	**40-60-0**	34-66-0 56-43-0
07OD47D2 1 layer	3	**26-74-0**	
07OD49C 3 layers	3	**36-49-15**	44-56-0 22-17-61 13-86-1
10OM26-2 3 layers	3	**7-91-2**	7-91-1 2-96-2 14-82-4
10OM43A 1 layer	3	**11-88-1**	
07OD48 3 layers	4	**46-28-26**	3-76-21 68-11-21 37-26-37
07OD47B1 2 layers	4	**9-61-30**	8-53-39 11-89-0
07OD47B3 2 layers	4	**43-40-15**	69-19-12 15-65-20
07OD47A 2 layers	4	**40-58-2**	12-87-1 95-3-2
10OM43L 3 layers	4	**23-77-0**	27-71-1 7-93-0 37-63-0
10OM26-4 3 layers	4	**10-83-7**	14-76-10 1-96-3 12-82-6